

Appendix A. The Novel ZVT and ZCT Soft-Switching Topology

Since the PCS needs to handle high power high voltage, the soft-switching topologies utilized in the design should have both ZVT and ZCT functions. A novel soft-switching topology that has both ZVT and ZCT functions is suggested.

The new topology has both ZVT and ZCT functions by using two additional components, a switch and a diode. The auxiliary inductor for soft-switching is implemented inside the main inductor with a tap. This concept can be applied to the isolated converters, the converters for the inductive load, and the three-phase converters/rectifiers.

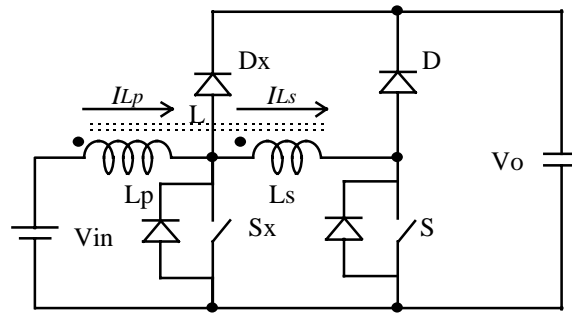


Figure A-1. An example of a PWM boost converter with a tapped inductor.

A.01 The Operation Principle

An example of a PWM boost converter of the proposed topology is shown in Figure A-1. A switch S , a diode D , and an inductor L make up a boost converter. The auxiliary switch S_x and the diode D_x are connected to the tap of inductor L . The inductor L can be divided into two inductors, the primary side L_p and the secondary side L_s , with a coupling constant K . The leakage inductance of L_s can be expressed as follows:

$$(A-1) \quad L_{sleak} = (1-K) \cdot L_s$$

and corresponds to the auxiliary inductor of the ZVT converter[12].

(a) ZVT Operations

Figure A-2 shows the operation stages and Figure A-3 shows key waveforms of the sample converter. Initially, the inductor current flows through diode D .

1) t_0 - t_1 : This is the first stage of the turn-on process. At t_0 , the auxiliary switch S_x is turned on, and its current I_{s_x} starts to build, reducing the main diode current I_D . The relationship between this time and the primary and secondary side currents of the tapped inductor, I_{L_p} and I_{L_s} , can be expressed as follows:

$$(A-2) \quad I_p(t) = I_p(t_0) + \left(\frac{I}{n} \cdot \frac{(V_o + V_{in}/n)}{L_{sleak}} + \frac{V_{in}}{L_p} \right) \cdot (t - t_0);$$

$$(A-3) \quad I_s(t) = I_p(t_0) - \frac{(V_o + V_{in}/n)}{L_{sleak}} \cdot (t - t_0); \text{ and}$$

$$(A-4) \quad I_{s_x}(t) = I_p(t) - I_s(t) = \left(\frac{(1+n)}{n} \cdot \frac{(V_o + V_{in}/n)}{L_{sleak}} + \frac{V_{in}}{L_p} \right) \cdot (t - t_0).$$

The length of this time is

$$(A-5) \quad t_{01} = \frac{I \cdot L_{sleak}}{(V_o + V_{in}/n)},$$

where I is the inductor current at t_0 .

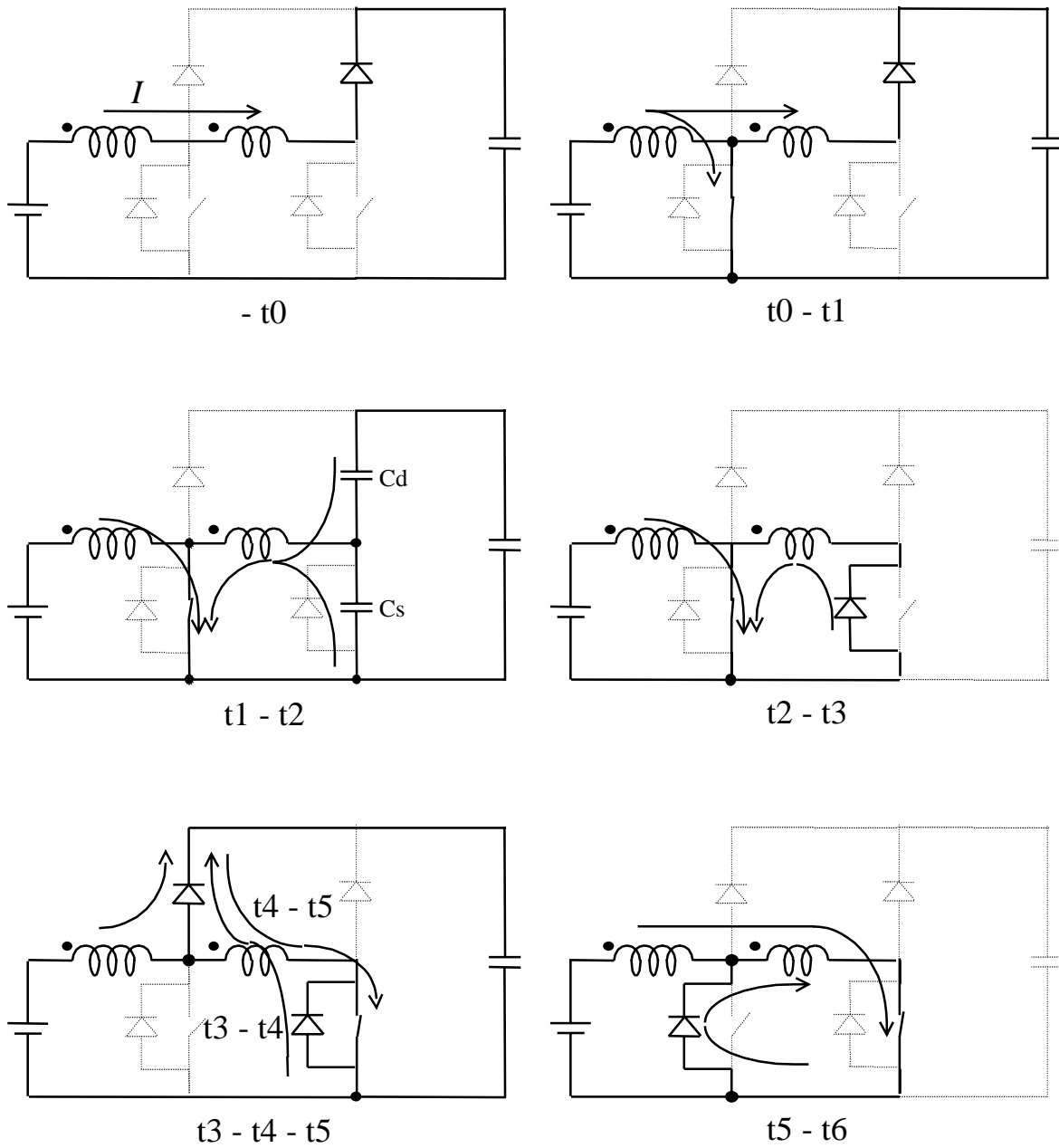


Figure A-2. The operation stages

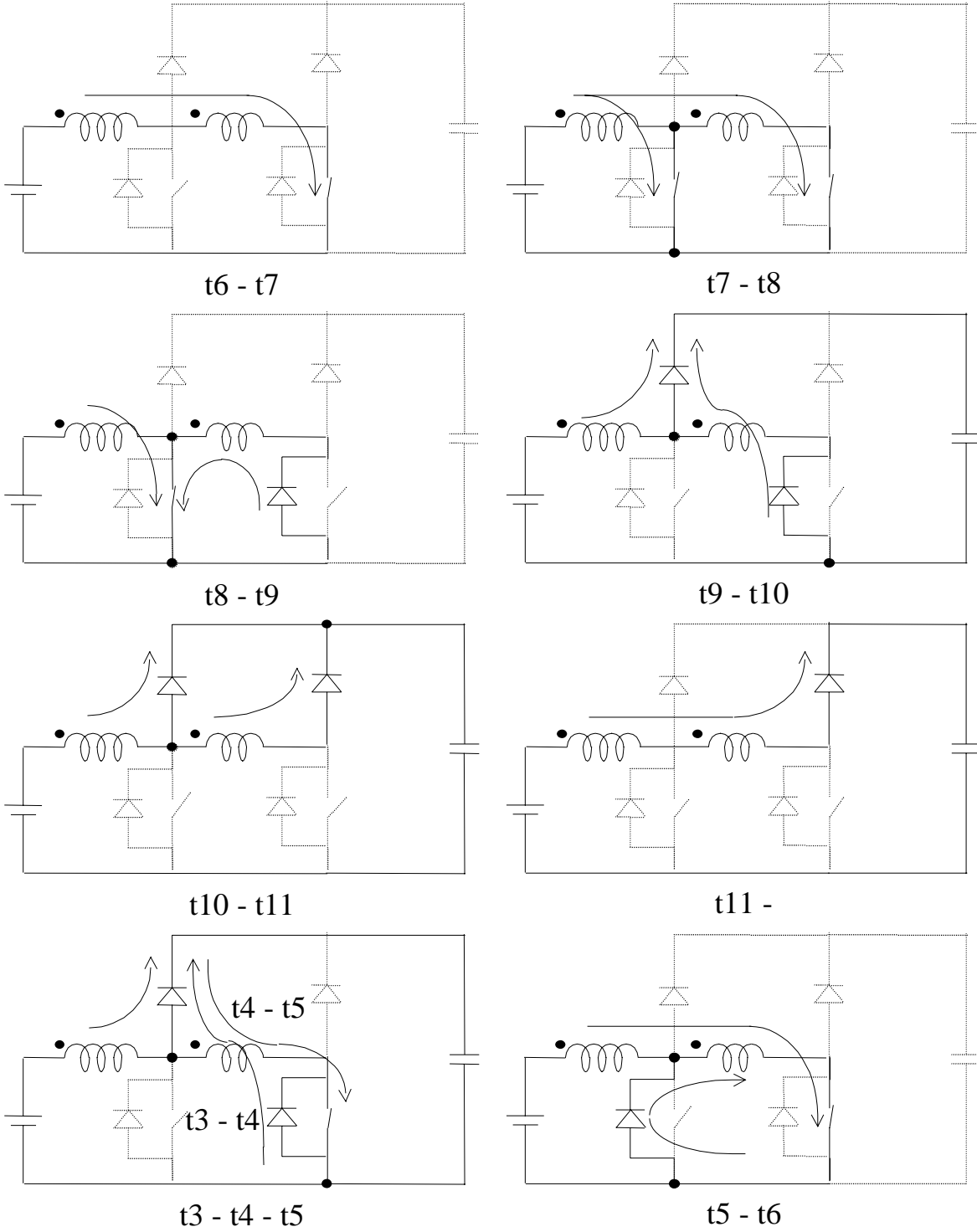


Figure A-2 (Continued). The operation stages

2) t_1 - t_2 : t_1 is the time when the main diode D is turned off. At this stage, the current I_{Ls} starts to resonate with the L_{sleak} and the parasitic capacitors of the main switch C_s and the main diode C_d . This stage ends when the anti-parallel diode of the main switch begins to conduct. The length of this time is approximately a quarter of the resonance period of the parasitic capacitors and the L_{sleak} , and is represented as follows:

$$(A-6) t_{12} \cong \frac{2\pi\sqrt{L_{sleak} \cdot (C_s + C_d)}}{4} \quad \text{if } V_o \gg V_{in}/n.$$

When there is no anti-parallel diode at the main switch, resonance starts at t_2 between the L_{sleak} and the $C_s + C_d$ (assume $C_o \gg C_d$), with induced voltage across L_s that is V_{in}/n . The peak-to-peak voltage of the resonance will be from zero to $-2V_{in}/n$.

3) t_2 - t_3 : After turn-on of the anti-parallel diode of the main switch, the current still increases, but the slope is determined by the secondary voltage of the tapped inductor. During this period, the main switch can be turned on with zero voltage. At t_3 , the auxiliary switch S_x is turned off. The length of this time can be minimized as long as the main switch is turned on. If an IGBT with no anti-parallel diode is used as the main switch, there is no current flow during this time. Instead of the current flow, the main switch sees the negative voltage across it. The amount of the voltage will be $-V_{in}/n$.

4) t_3 - t_5 : After turn-off of the auxiliary switch, the currents I_{Lp} and I_{Ls} continue to flow through the auxiliary diode and start to be reset by the output voltage and the secondary-side voltage of the tapped inductor. The time from t_3 to t_4 is represented as follows:

$$(A-7) t_{34} = \frac{I_s(t_3) \cdot L_{sleak}}{(V_o + (V_o - V_{in})/n)}.$$

t_4 is the time when $I_{L_s} = I_{L_p}$. After t_4 , the auxiliary diode D_x starts to recover. Therefore, the time t_5-t_4 is the reverse recovery time of the auxiliary diode.

5) t_5-t_6 : At t_5 , the secondary side current I_{L_s} becomes greater than the I_{L_p} due to the reverse recovery of the auxiliary diode. This current again starts to be reset by the secondary voltage of the tapped inductor.

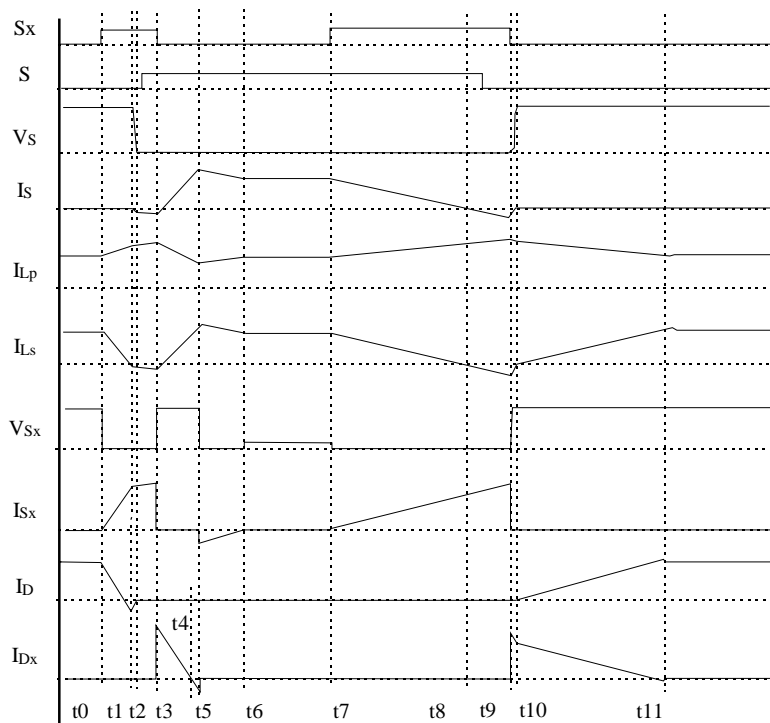


Figure A-3. Key waveforms

6) t_6-t_7 : Time t_6 is the end of the turn-on process. This is the switch-on period of the PWM. The length of time is determined by the control of the PWM.

The actual switch-on period starts at t_0 in terms of the PWM switching. So, the time period from t_0 to t_6 is the duty ratio limit for turn-on.

(b) ZCT Operations

1) t_7 - t_9 : From t_7 , the turn-off process starts. The current I_{Ls} starts to decrease with the aid of the secondary voltage of the tapped inductor:

$$(A-8) \quad t_{78} = \frac{I \cdot L_{sleak}}{V_{in}/n},$$

where I is the inductor current at t_7 .

At t_8 , the current I_{Ls} changes its direction and flows through D_s , the anti-parallel diode of the main switch. After t_8 , the main switch can be turned off with zero current. At t_9 , the auxiliary switch S_x is turned off. The length of this time should be long enough for full turn-off of the main switch, so this should depend on the switch characteristics. Together with the time period t_0 to t_6 , this time is also the duty ratio limit for the PWM.

2) t_9 - t_{10} : During this period, the current I_{Ls} flows through the anti-parallel diode of the main switch, and drops rapidly due to the output voltage and the secondary-side voltage of the tapped inductor.

3) t_{10} - t_{11} : The current I_{Ls} starts to build until $I_{Ls} = I_{Lp}$ with the aid of the secondary side voltage of the tapped inductor. This time is another duty ratio limit for the switch-off period of the PWM.

4) t_{11} - : The turn off process finishes at t_{11} . This is the PWM turn-off period.

A.02 A Three-Level Topology

With modifications of the PWM switch cell as shown in Figure A-4, the concept of the ZVT and ZCT functions can be extended to the three-level topology, as shown in Figure A-5.

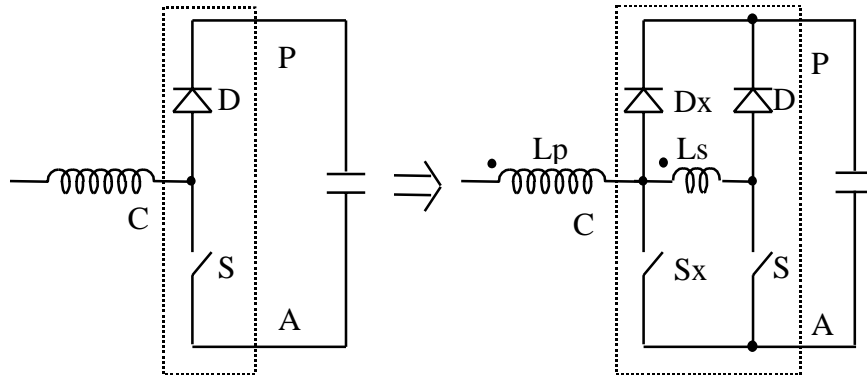


Figure A-4. The changes in the PWM switch cell

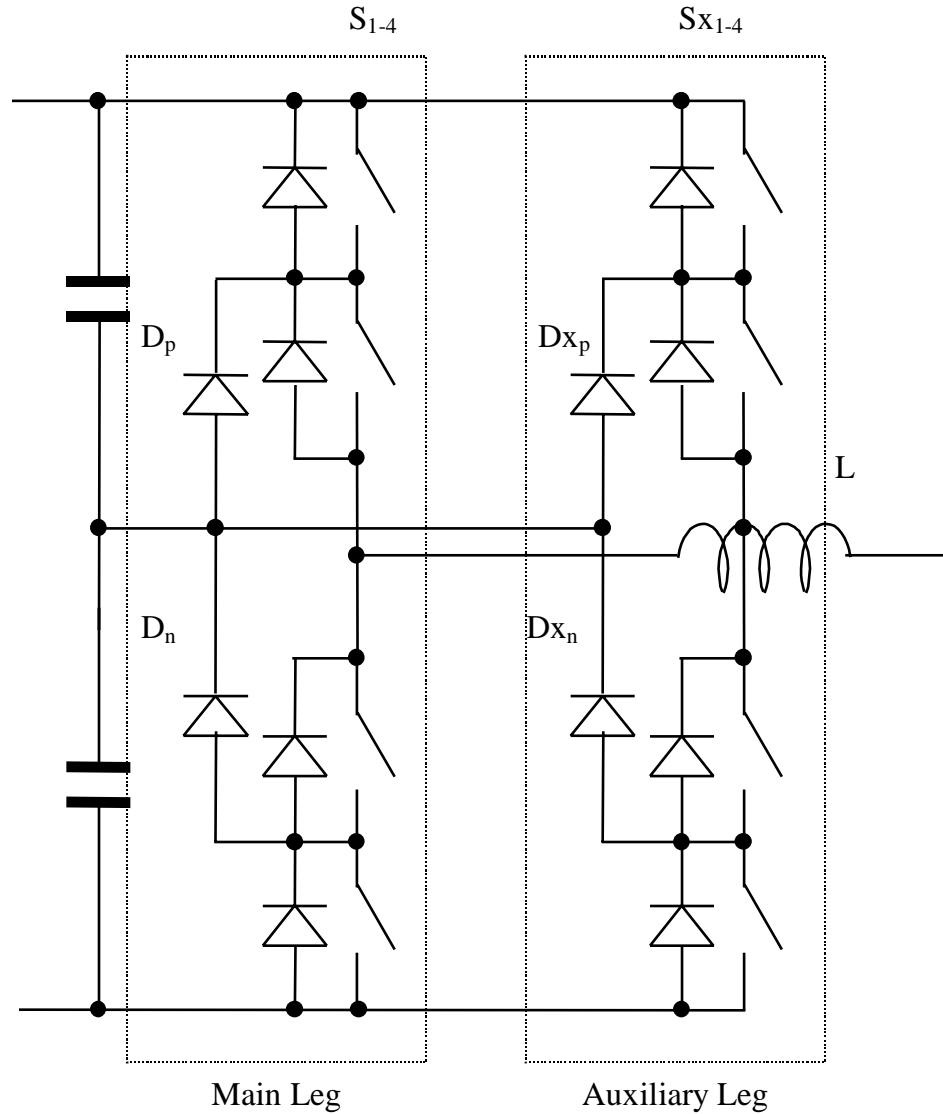


Figure A-5. The three-level implementation of the ZVT and ZCT topology

A.03 A Novel Soft-Turn-On and ZCT Soft-Switching Topology

The proposed ZVT and ZCT PWM converter topology can be further simplified by eliminating the auxiliary diode and moving the main diode to the auxiliary diode position. Figure A-6 shows a basic boost converter of this topology. The major difference of this modified topology in terms of circuit operation is that it does not have the ZVT operation. However, due to the leakage inductance of the secondary side of the main inductor

between the diode and the main switch, this new topology does not have the reverse recovery problem of the main diode. This function can be called soft-turn-on, and this topology can be called the soft-turn-on and ZCT topology. Circuit parameters, such as primary and secondary inductors, the coupling constant, and turn ratio, are the same as those of the ZVT and ZCT converter case.

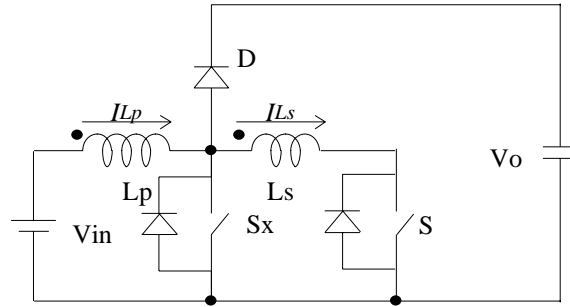


Figure A-6. An example of the modified topology boost converter

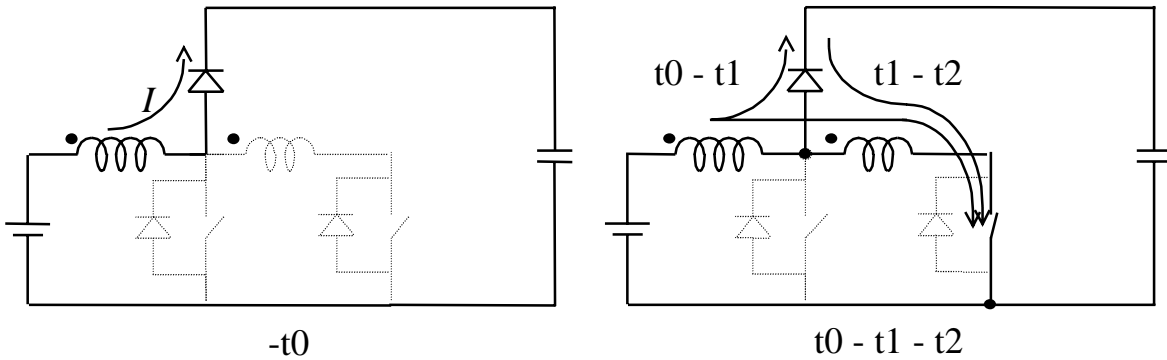


Figure A-7. The operation stages

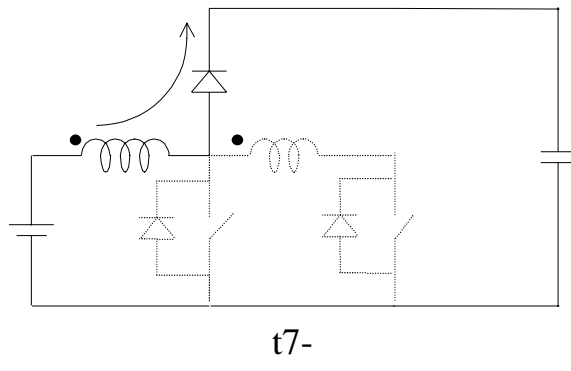
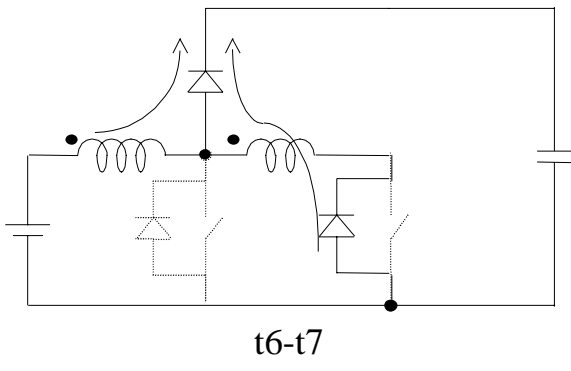
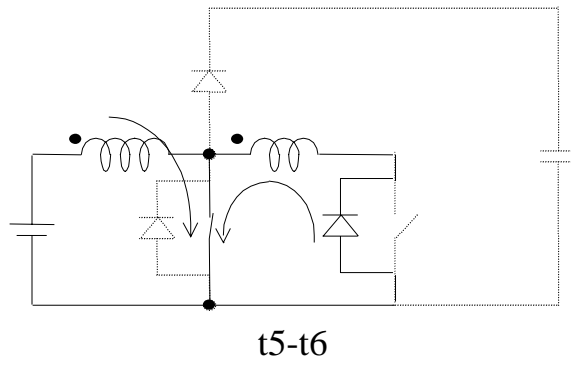
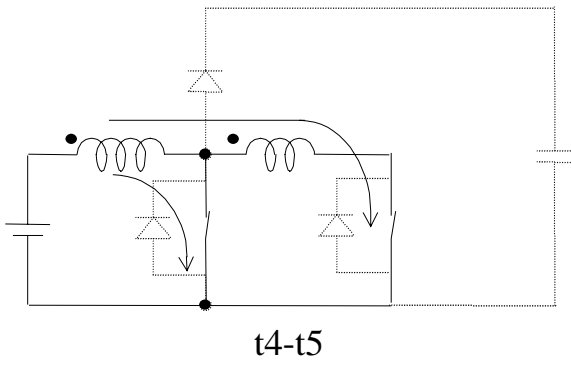
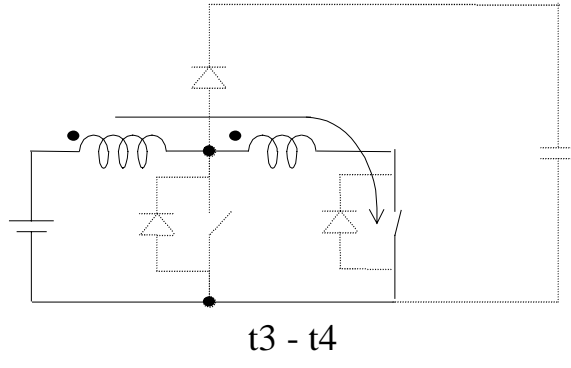
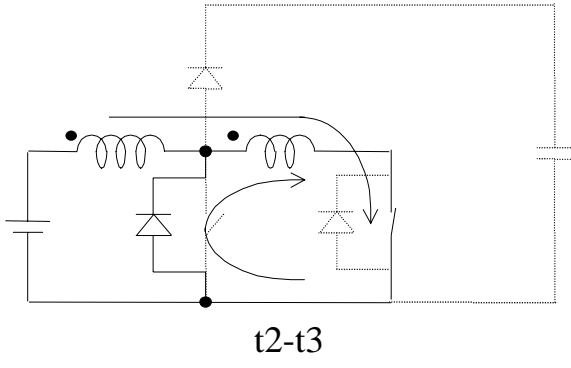


Figure A-7 (Continued). The operation stages

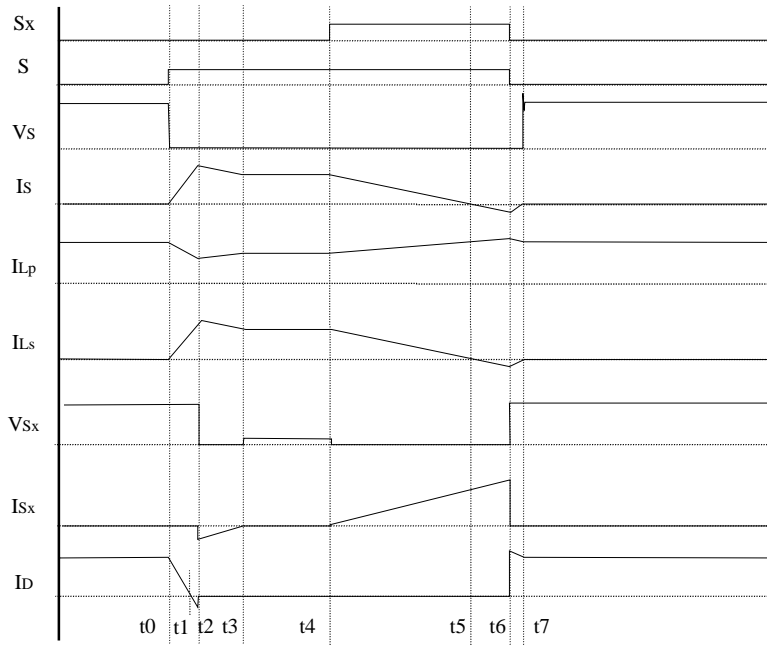


Figure A-8. Key waveforms

(a) Circuit Operations

Figure A-7 shows the operation stages and Figure A-8 shows its key waveforms of the sample converter. Initially, the inductor current flows through the diode D .

1) t_0 - t_2 : This is the first stage of the turn-on process. At t_0 , the main switch is turned on and the current I_{Ls} starts to build, reducing the main diode current. The length of this time is

$$(A-9) \quad t_{01} = \frac{I \cdot L_{sleak}}{(V_o + (V_o - V_{in})/n)},$$

where I is the tapped inductor current at t_0 .

The t_1 is the time when the main diode current I_D changes its direction. The time between t_1 and t_2 is the reverse recovery time of the main diode.

2) t_2 - t_3 : After turn-off of the main diode, the excessive current caused by the reverse recovery of the main diode flows through the anti-parallel diode of the auxiliary switch. This current is reset by the secondary voltage of the tapped inductor. Different from the ZVT and ZCT converter case, t_0 is the start of the PWM turn-on period. So, the time period from t_0 to t_3 is the duty ratio limit for the turn-on period of the PWM.

3) t_3 - t_4 : The time t_3 is the end of the turn-on process. This period is the switch-on period of the PWM. The length of time is determined by the control of the PWM.

4) t_4 - t_6 : From t_4 , the turn-off process starts. The current I_{Ls} starts to decrease due to the secondary voltage of the tapped inductor. The current I_{Ls} and the length of the time can be expressed as follows:

$$(A-10) \quad I_s(t) = I_s(t_4) - \frac{V_{in}/n}{L_{leak}} \cdot (t - t_4), \text{ and}$$

$$(A-11) \quad t_{45} = \frac{I \cdot L_{leak}}{V_{in}/n},$$

where I is the tapped inductor current at t_4 .

At t_5 , the current I_{Ls} changes its direction and flows through D_s , the anti-parallel diode of the main switch. After t_5 , the main switch can be turned off with zero current. At t_6 , the auxiliary switch S_x is turned off. The length of this time should be long enough for full turn-off of the main switch, so this should depend on the switch characteristics. The time t_5 to t_6 should be kept small enough to prevent the current I_{Ls} from flowing to the

negative direction. This will reduce ringing after t_6 . These times are also another duty ratio limit for the PWM. The total duty ratio limit is $t_{03} + t_{46}$.

5) t_6 - t_7 : During this period, the current I_{L_s} flows through the anti-parallel diode of the main switch, and drops rapidly due to the output voltage and the secondary side voltage of the tapped inductor. This time is zero when the main switch current is kept at zero during the t_5 - t_6 period.

6) t_7 -: The current I_{L_p} flows through the main diode. The turn-off process finishes at t_7 . This period is the switch-off period of the PWM. The turn-off duty ratio limit is t_6 - t_7 for this topology.

(b) The Three-Level Topology

With modifications of the PWM switch cell, as shown in Figure A-9, the concept of the soft-turn-on and ZCT can be extended to the three-level topology as shown in Figure A-10.

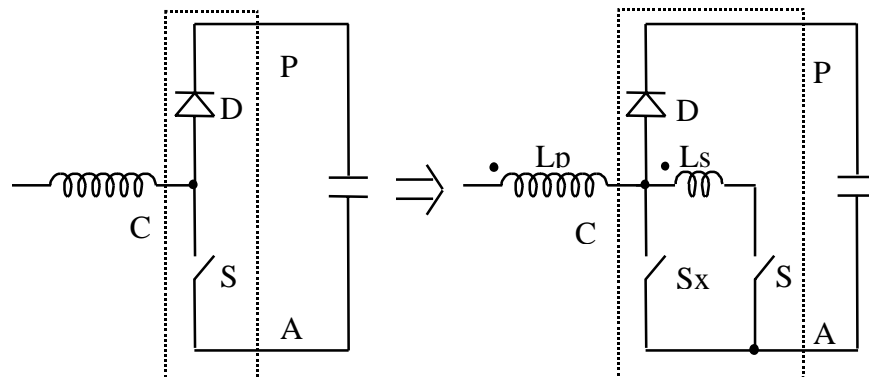


Figure A-9. The changes in the PWM switch cell

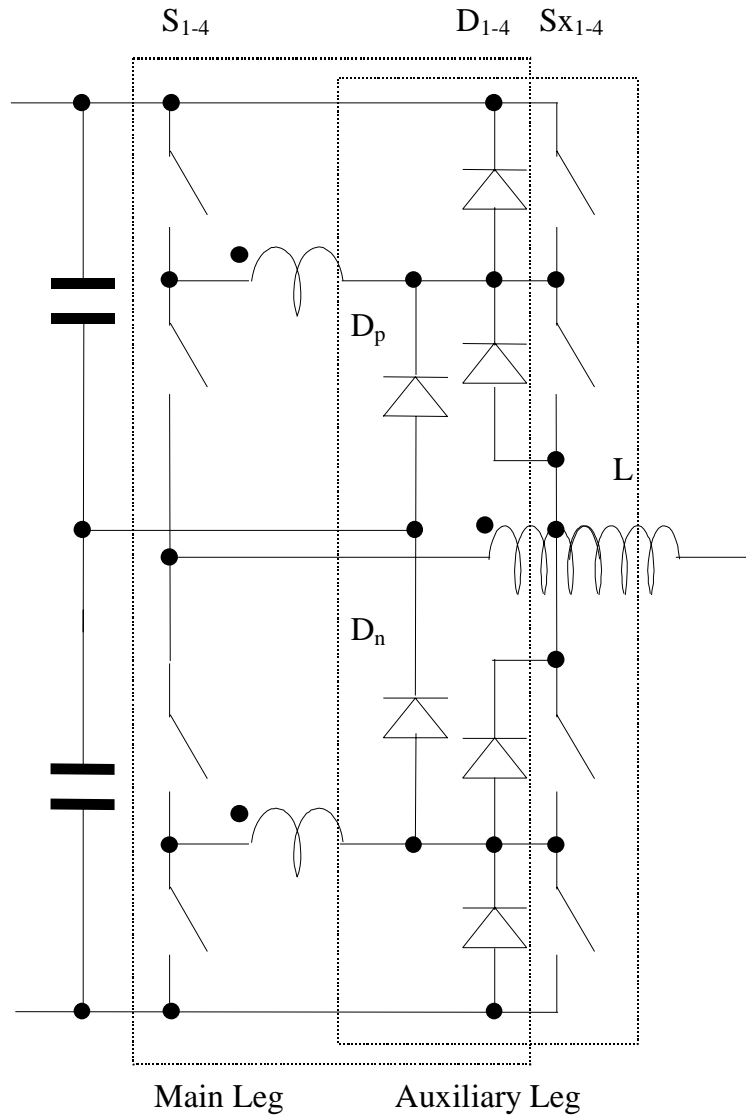


Figure A-10. The three-level implementation of the soft-turn-on and ZCT topology

A.04 Design Considerations

As with the operational principle, the role of the tapped inductor is very important; not only the position of the tap needs consideration, but also the coupling constant of the inductor matter. The position of the tap, together with the coupling constant, will

determine the slope of the current increase/decrease during the turn-on/off processes. The auxiliary switch turn-on time is linearly proportional to the inductor current with the given slope. In addition, the position of the tap will determine the amount of the voltage across the leakage inductance of the secondary side of the tapped inductor. Following are the design processes of those circuit parameters. The first step is the determination of the value of the leakage inductance. The second step is the determination of the turn ratio, The third step is the determination of the coupling constant. In this design, it is assumed that the input voltage V_{in} and the output voltage V_o are fixed.

(a) Leakage Inductance

The value of the leakage inductance of the secondary side of the tapped inductor, together with the voltage across it, determine the slopes of the current change during the turn-on and turn-off processes, as mentioned before. During the turn-on time, from t_0 to t_2 , as shown in Figure A-3, the voltage across the leakage inductance is

$$(A-12) \quad V_{L_{leak}} = \frac{I}{n}((n-1) \cdot V_o + V_{in}).$$

During the turn-off time, from t_7 to t_{10} , the voltage is only V_{in}/n . As the turn ratio becomes larger, the voltage during the turn-on process approaches the output voltage V_o , while during turn-off, it becomes very small. Therefore, the turn-on slope mainly depends on the value of the leakage inductance. The required amount of time for the turn-on process of the PWM converter depends quite strongly on the reverse recovery characteristics of the main diode, the turn-on characteristics of the main switch, the inductor current, and the circuit parasitic. Usually, in terms of the voltage and current

spikes, the longer the turn-on time, the better. In terms of the duty ratio limit, the shorter the turn-on time, the better.

(b) Turn Ratio

Once the value of the leakage inductance has been determined, the next step is to determine the turn ratio of the tapped inductor. The turn ratio not only determines the secondary side voltage, which in turn determines the turn-off slope during the ZCT operation, but also influences the amounts of the ripple current in the inductor. As shown in Figure A-3, the primary-side current I_{Lp} is changed due to the secondary-side current by the transformer action of the tapped inductor. The polarity of the ripple, during the turn-on stages from t_0 to t_6 as shown in Figure A-3, is opposite to that of the primary current ripple. In contrast, at the turn-off stages from t_7 to t_{11} as shown in Figure A-3, they have the same polarity, resulting in the increase of the ripple. The amount of this additional current ripple at the primary side is I_{Ls}/n . So, the larger the turn ratio, the smaller the ripple. For the turn-off process, the peak value of the inductor current will be

$$(A-13) \quad I_{peak} = I \left(1 + \frac{r}{2} \right) \left(1 + \frac{1}{n} \right),$$

where r is the ratio of the ripple current to the average DC current through the inductor.

(c) Coupling Constant

With the given value of the leakage inductance and the turn ratio, the coupling constant is the only factor that can give the desired slope during the turn-off stages. The turn-off time, from t_7 to t_{10} as shown in Figure A-3, should be determined by the main switch

turn-off characteristics. With the maximum load current, this time determines the slope. The slope, together with the given leakage inductance, L_{leak} , and the inductor L , determines the coupling constant K and turn ratio n as follows:

$$(A-14) \quad L_{leak} = \frac{L}{n^2} \cdot (1 - K).$$

A.05 Experimental Result

A simple prototype 2-kW boost DC-DC converter was built to verify the operation and efficiency improvements of the ZVT/Soft-Turn-On and the ZCT topology. Figure A-11 shows the prototype converter for measuring efficiency. The components used were as follows. For the main switch, a 600-V 50-A fast-IGBT from IR, IRGPC50F, and for the auxiliary switch, a 400 V 16 A 0.30 Ω MOSFET from IR, IRFP350, were used. A fast recovery diode from Philips, BYV44, which is 500-V 30-A 50-nsec, was used. For the auxiliary diode, a 400-V 3-A 30-nsec fast-recovery diode from IR, 31DF4, was used. The turn ratio was set to six. The number of turns at the primary side was eighteen, and at the secondary side was three. The switching frequency was 20-kHz.

Gate drive signals for the two switches were synthesized using an arbitrary signal generator. The time delays between the auxiliary switch and the main switch were set manually to find the best operating points.

Figure A-12 and 14 show the experimental waveforms of the prototype converter with different conditions. The component values and devices used are different from those shown in Figure A-11. Figure A-12 shows the waveforms with the low coupling constant tapped inductor, and Figure A-13 shows that of the high coupling constant tapped

inductor. Figure A-14 shows the soft-turn-on and ZCT converter case with the high coupling constant. In this case, the main diode was moved to the auxiliary diode position. At the main diode position, another diode from IR, 31DF4, and a 1-W 25-V Zener diode were connected in series, as shown by the dotted line diodes in Figure A-11. The reason for doing this is to clamp the voltage across the main switch within the maximum limit, in case of turn-off with non-zero current at the secondary inductor. The first and the second waveforms are the voltage and current of the main switch. The third and the fourth waveforms are those of the auxiliary switch. The scaling factor of the second and the fourth waveforms is 40 A/div.

Figure A-15 shows the efficiency improvements. The efficiency is improved throughout all ranges of the load. The soft-turn-on and ZCT topology is more efficient than the ZVT and ZCT topology. This is due to the number of turn-off actions of the auxiliary switch. Even though the soft-turn-on and ZCT topology has better performance and needs fewer extra components than the ZVT and ZCT topology, it suffers voltage ringing at the end of the turn-off process. This is caused by the reverse current flowing through the L_s after resetting to charge the parasitic capacitance of the auxiliary switch. This makes this topology somewhat more difficult to use than the ZVT and ZCT topology. In the experiment, a diode and a 25-V Zener diode were used to clamp the voltage ringing, as shown in Figure A-11.

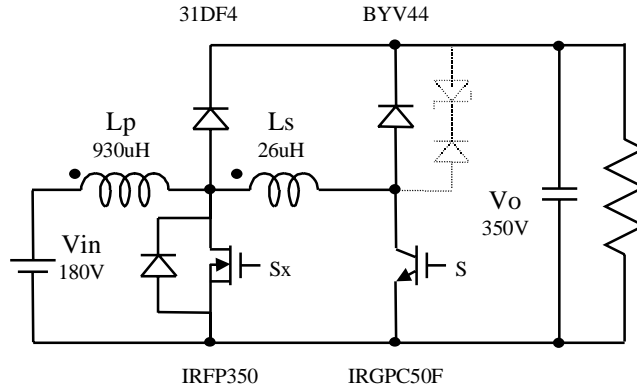


Figure A-11. An experimental boost converter with a tapped inductor

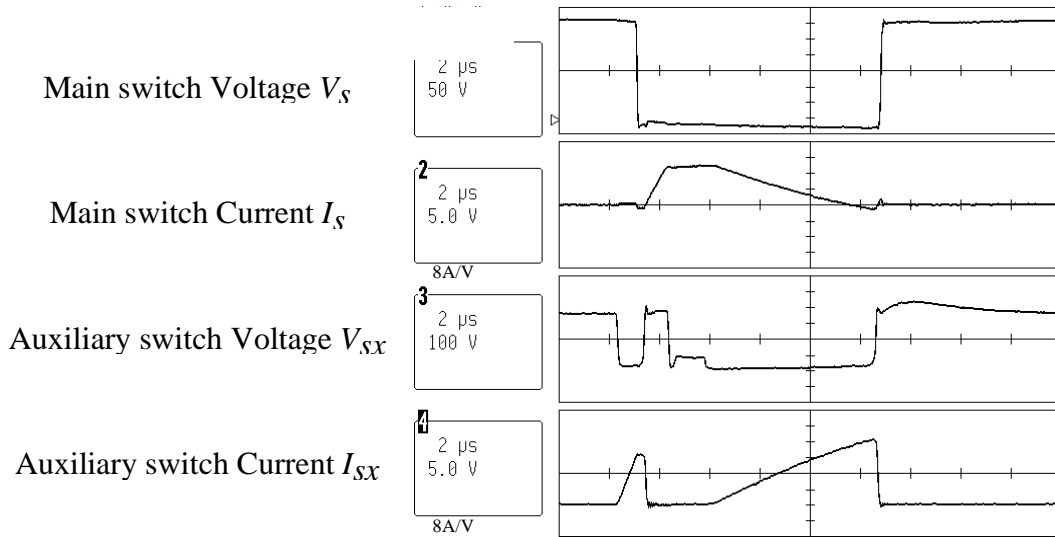


Figure A-12. Experimental waveforms of the ZVT and ZCT boost converter with a low K inductor

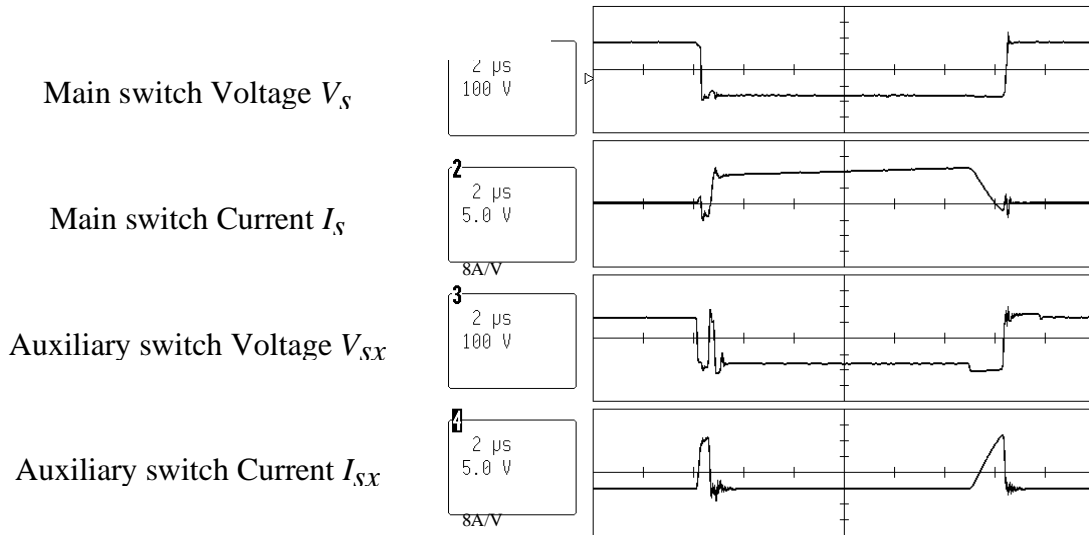


Figure A-13. Experimental waveforms of the ZVT and ZCT boost converter with a high

K inductor

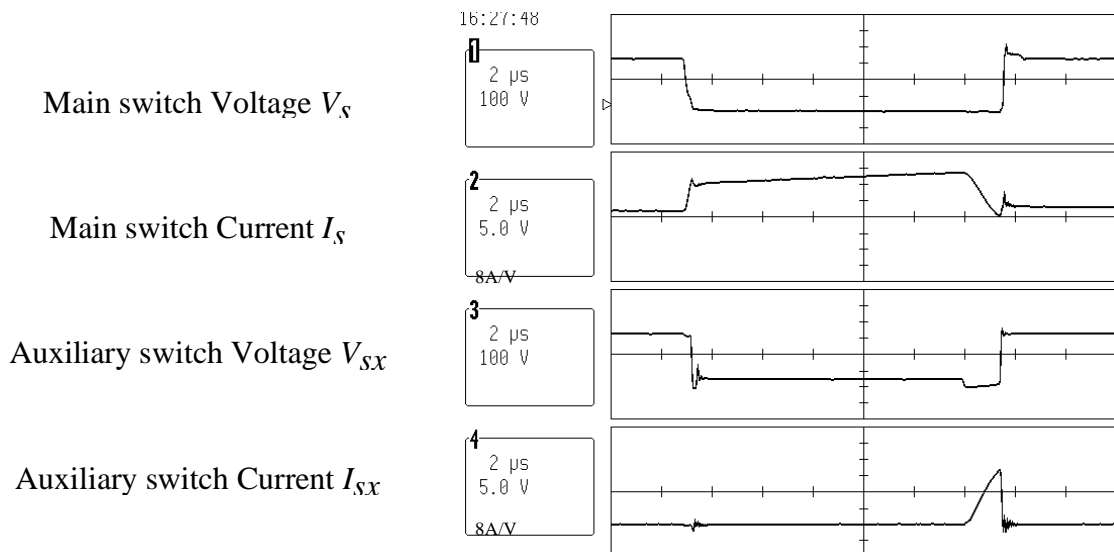


Figure A-14. Waveforms of the soft-turn-on and ZCT boost converter

The disadvantages of the topologies are a hard turn-off of the auxiliary switch and additional ripple in the inductor current, when the auxiliary inductor is implemented at the main inductor.

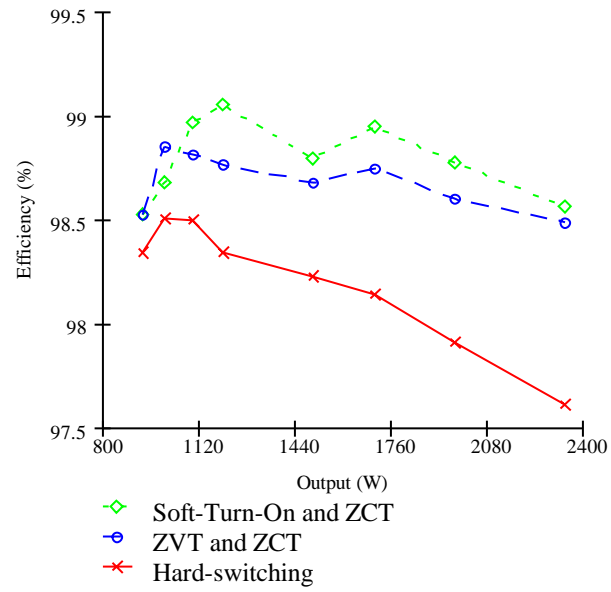


Figure A-15. Efficiency comparison of the boost converter with different switching topologies.